Solvent Distribution in Weakly-Ordered Block Copolymer Solutions

Timothy P. Lodge,*,† Mark W. Hamersky,‡ Kenneth J. Hanley,‡ and Ching-I Huang*,‡

Department of Chemistry and Department of Chemical Engineering & Materials Science, University of Minnesota, Minneapolis, Minnesota 55455-0431

Received May 23, 1997; Revised Manuscript Received July 25, 1997[⊗]

ABSTRACT: The distribution of solvent in block copolymer solutions near their order−disorder transitions is examined experimentally, by small-angle neutron scattering (SANS), and theoretically, by the self-consistent mean-field (SCMF) approach. Three lamellar-forming poly(styrene-*b*-isoprene) diblocks were employed, in toluene, a neutral good solvent, and in cyclohexane, a selective solvent. For a given copolymer concentration, two solutions were prepared, one in protonated and one in perdeuterated solvent, and the scattering profiles compared. For a neutral solvent, one expects a small partitioning of the solvent to the interface between microdomains, to screen unfavorable styrene−isoprene contacts. Such partitioning should be manifest as a difference between the *h*- and *d*-solvents in the intensities of the second (and higher order, even) harmonic peaks (i.e., $I(2q^*)$, where the lamellar spacing, L, is $2\pi/q^*$). This difference is observed experimentally, and is in quantitative agreement with SCMF predictions using literature values for the three interaction parameters. Interestingly, the predicted relative scattering intensity between solutions in *h*- and *d*-toluene varies by several orders of magnitude over a small range in copolymer composition or over a small range of relative interaction parameters of the solvent for the two blocks, suggesting that SANS could be used in this way as a very sensitive measure of copolymer composition and/or solvent selectivity. For a selective solvent, one expects partitioning of the solvent between microdomains and a concomitant change in the intensities of the primary (and higher order, odd harmonic) peaks between *h*- and *d*-solvents. This effect is seen clearly in cyclohexane, with the partitioning of the solvent into the isoprene domains increasing with decreasing temperature. However, the SCMF calculations can only match the behavior in both solvents by employing polyisoprene−cyclohexane and polystyrene−cyclohexane interaction parameters significantly different from those reported in the literature.

Introduction

Block copolymer phase behavior continues to be a subject of great interest. Yet, less attention has been directed to concentrated block copolymer solutions, where one may anticipate interesting effects of chain swelling and solvent selectivity. Furthermore, the presence of two compositional order parameters (e.g., block A vs block B and polymer vs solvent) enriches the range of structural possibilities. For example, a neutral solvent should distribute itself equally between the two microdomains, whereas even a very slight degree of selectivity could lead to a measurable preferential swelling of one component. In either case, the solvent could collect in the interfacial region between microdomains, in order to screen unfavorable A−B interactions. As far as we are aware, these issues of solvent distribution in concentrated block copolymer solutions have not been examined experimentally, although studies on the related problem of swelling of thin block copolymer films have recently appeared.[1,2]

Theoretical studies of the phase behavior of nondilute block copolymer solutions have considered two regimes.[3−7] In the concentrated limit, a "dilution approximation" has been invoked,[8] whereby the primary effect of added neutral solvent is to screen A−B contacts in a spatially uniform manner. Consequently, the state of the system is assumed to be governed by $\phi\chi N$, where ϕ is the polymer volume fraction, χ is the A−B interaction parameter, and N is the total degree of polymerization. In particular, for a given copolymer composition, f, the mean-field order−disorder transition (ODT) is located by $(\phi\chi N)_{ODT} = F(f)/2$ (with $F(0.5) = 21$), and the melt results are simply recovered by setting $\phi = 1$. At fixed temperature, therefore, the ordering concentration ϕ_{ODT} scales as N^{-1}. The self-consistent mean-field theory retains this scaling, while predicting a slight segregation of solvent to the A−B interface.[5,7] In semidilute solutions, chain swelling cannot be ignored. Olvera de la Cruz[6] and Fredrickson and Leibler[5] have considered this regime, essentially by treating the system as a melt of blobs. Scaling laws for the concentration dependence of the blob size and the effective interaction parameter between blobs[9,10] lead to the result $(\phi^{1.59}\chi N)_{ODT} = cF(f)/2$, with c a constant of order unity, and thus the prediction that at a fixed temperature ϕ_{ODT} scales as $N^{-0.62}$.

Experimental studies of concentrated block copolymer solutions have emphasized nominally neutral solvents, such as toluene and dioctyl phthalate in the case of styrene−isoprene (SI) copolymers. The first systematic studies of this type were performed by Hashimoto and co-workers.[11,12] These results, and others on similar or related systems, have tacitly invoked the dilution approximation but without testing it directly. Recently, we examined the location of the ODT for symmetric SI copolymers as a function of N in these two solvents and found that the predicted semidilute scaling, $\phi_{ODT} \sim N^{-0.62}$, was followed from $\phi = 0.14$ all the way up to the melt.[13] Thus, in these systems there is apparently no regime of validity of the dilution approximation. The fact that the exponent follows the semidilute prediction is probably coincidental, but the substantial deviation from mean-field theory is clear; the addition of solvent is more effective at stabilizing the disordered state than

* To whom correspondence should be addressed.
† Department of Chemistry.
‡ Department of Chemical Engineering & Materials Science.
⊗ Abstract published in *Advance ACS Abstracts,* September 1, 1997.

S0024-9297(97)00720-1 CCC: $14.00

Table 1. Sample Characteristics

sample	M_{PS}	M_{PI}	f	M_w/M_n
SI(16-19)	1.6×10^4	1.9×10^4	0.43	1.06
SI(41-45)	4.1×10^4	4.5×10^4	0.44	1.06
SI(10-13)	1.0×10^4	1.3×10^4	0.40	1.05

expected. A variety of factors not considered in mean-field theory may be implicated, including chain stretching, enhanced solvent screening of interactions, and substantial fluctuations in either or both order parameters. A recent application of PRISM theory is successful in accounting for these results, and ascribes them to nonuniversal, nonrandom mixing.[14]

One factor that may be addressed directly is the distribution of solvent. In this paper we develop the use of small-angle neutron scattering (SANS) to investigate the solvent distribution in block copolymer solutions near the ODT. Three nearly symmetric SI diblocks have been used, with toluene as a nominally neutral solvent and cyclohexane as a representative selective solvent. For a given polymer and concentration, two solutions have been examined: one with the protonated solvent and one with its perdeuterated analog. Differences in the scattering function between the two solutions are thus directly attributable to spatial correlations in solvent distribution. In the case of toluene, the results reveal a small, but distinct segregation of the solvent to the interface and a slight preference toward swelling of the isoprene-rich domains. The cyclohexane results indicate a strong temperature-dependent preferential swelling of the isoprene domains. Self-consistent mean-field theory has been employed to provide a more quantitative interpretation of the data and to calculate the corresponding equilibrium composition profiles.

Experimental Section

Samples and Solutions. The three nearly symmetric poly(styrene-*b*-isoprene) (PS−PI) diblock copolymers used in this study were synthesized by sequential living anionic polymerization. Solvents, monomers, and reagents were purified using established procedures.[15,16] In each case, the styrene block was polymerized first using *sec*-butyllithium as the initiator. The solvent was benzene in two cases and cyclohexane in the third; the resulting molecular weights of the copolymers are 8.6×10^4, 3.5×10^4, and 2.3×10^4, respectively. The copolymer molecular weights and compositions were determined by standard procedures, as previously described.[15,16] The volume fractions of PS, f, were calculated using densities of 1.04 and 0.913 g/mL for PS and PI, respectively. The characterization data are listed in Table 1, and the samples are designated SI(41-45), SI(16-19), and SI(10-13), where the numbers refer to the block molar masses in kg/mol.

Solutions were prepared gravimetrically using toluene, cyclohexane, and their perdeuterated versions. All solvents were used as purchased from Aldrich. A weighed amount of copolymer was placed in a cell that consists of two quartz disks (1 in. dia.) circumferentially fused with a 1.0 mm gap, except for a small tube (5 mm o.d.) to permit filling. The appropriate amount of solvent was added along with a small amount (0.2−0.5 wt % relative to polymer) of 2,6-di-*tert*-butyl-4-methylphenol (BHT) as an antioxidant. Solutions for each polymer and concentration were made as matched pairs (in polymer weight fraction), one with the hydrogenated and one with the perdeuterated solvent. Concentrations were chosen to include one sample near the order−disorder transition and three in the (lamellar) ordered state at room temperature, except for the SI(10-13) case where the material quantity was limited. The completed cells were sealed with a PTFE stopper that fit tightly in the filling neck of the cell and then annealed for approximately 24 h at 60 °C to aid in dissolution and equilibration. All samples were kept at room temperature for approximately 1 week prior to scattering experiments. Cell weights were monitored before and after scattering experiments to ensure concentration integrity. Solutions that were in the ordered state at room temperature developed some long-range orientation over time, as evident from the initial scattering patterns. These were heated into the disordered state and quenched, prior to the measurements to be described, in order to eliminate the preferential orientation.

Small-Angle Neutron Scattering. Small-angle neutron scattering (SANS) experiments were performed at the National Institute of Standards and Technology (NIST) in Gaithersburg, MD, using the 30 m SANS (NG7) instrument configured with a wavelength, λ, of 7 Å and a dispersion, $\Delta\lambda/\lambda$, of 0.10. Source and sample apertures were 50.0 and 9.5 mm, respectively. The sample-to-detector distance was fixed at either 4 or 6 m, depending on the sample and minimum q requirements, where q is the usual scattering vector ($=[4\pi/\lambda] \sin(\theta/2)$). To increase the high q limit of detection, the two-dimensional detector was offset by 15 cm horizontally. The sample temperature was controlled to within ±0.5 °C using either a circulation bath or resistive block heater. Temperatures were measured with a calibrated thermocouple immersed in a cell containing pure water, and the samples were equilibrated at the desired temperature for at least 15 min prior to measurement. In addition to the copolymer solution samples, SANS experiments were carried out on the protonated solvents and PS and PI homopolymers to make an estimate of the incoherent background. These data were independent of q, and the intensity in absolute units was averaged over the range $0.02 < q < 0.08$ Å^{-1}.

Data treatment was performed using NIST software. The data were corrected for transmission, sample thickness, background, and empty cell contributions. Additionally, the data were adjusted for detector sensitivity, azimuthally averaged, and placed on an absolute intensity scale using a calibrated silica standard (Sil A2) provided by NIST. An incoherent scattered intensity subtraction was applied to the data, based on solvent amount, type, and copolymer composition. A small positive scattering intensity persisted after this procedure, due presumably to a small Ornstein−Zernike-like scattering from the polymer−solvent structure factor, incoherent scattering from the deuterated solvent, and other uncertainties in the exact incoherent contribution. This residual intensity was removed by requiring that the intensity, averaged over the range $0.07 < q < 0.10$ Å^{-1}, be zero. The magnitude of these shifts was very small: typically 0.5% of $I(q^*)$ in absolute units, i.e., on the order of 0.1 cm^{-1}.

In order to compare the intensities of various peaks between two matched solutions, the advisability of desmearing the data was considered. Standard desmearing corrections were found to have significant effects on the peak intensity, $I(q^*)$, but it was not possible to establish a unique desmeared profile. However, it was found that peak areas were invariant to smearing and that ratios of smeared peak intensities gave results that were indistinguishable from ratios of the corresponding peak areas. Thus, the smeared peak intensities were employed. They were determined by fitting the data near the peak maximum to a Gaussian function, which also afforded reliable determination of the peak positions.

Results

For the analysis of the scattering functions in the lamellar ordered state, the fluctuations in composition about the mean may be expanded in a Fourier series as

$$\delta\phi_\alpha(\vec{r}) = \sum_{j=1} \varphi_{\alpha,j} \sqrt{2} \cos(jq^* r) \qquad (1)$$

where component α could be polystyrene (PS), polyiso-

Table 2. SANS Contrast Factors, $(a_\alpha - a_\beta)^2$, in Units of cm^{-1}

	PS	PI	*h*-toluene	*d*-toluene	*h*-cyclohexane	*d*-cyclohexane
PS	0	0.0216	0.00363	0.298	0.0471	0.467
PI	0.0216	0	0.00753	0.480	0.00491	0.689

prene (PI), or solvent (SOL) and q^* is the location of the first scattering peak. The incompressibility assumption requires that

$$\varphi_{\mathrm{SOL},j} + \varphi_{\mathrm{PS},j} + \varphi_{\mathrm{PI},j} = 0 \tag{2}$$

in addition to the relation for the mean ($j = 0$) volume fractions

$$\phi_{\mathrm{SOL}} + \phi_{\mathrm{PS}} + \phi_{\mathrm{PI}} = \phi_{\mathrm{SOL}} + \phi = 1 \tag{3}$$

The scattered intensity from the jth harmonic $I(jq^*)$ can, to within a multiplicative constant, be expressed as[17]

$$I(jq^*) = (a_{\mathrm{PS}} - a_{\mathrm{SOL}})^2 \varphi_{\mathrm{PS},j}{}^2 + (a_{\mathrm{PI}} - a_{\mathrm{SOL}})^2 \varphi_{\mathrm{PI},j}{}^2 + ((a_{\mathrm{PS}} - a_{\mathrm{SOL}})^2 + (a_{\mathrm{PI}} - a_{\mathrm{SOL}})^2 - (a_{\mathrm{PS}} - a_{\mathrm{PI}})^2)\varphi_{\mathrm{PS},j}\varphi_{\mathrm{PI},j} \tag{4}$$

where a_α is the scattering length density of component α. If the solvent is uniformly distributed, $\varphi_{\mathrm{SOL},j} = 0$, and

$$I(jq^*) = (a_{\mathrm{PS}} - a_{\mathrm{PI}})^2 \varphi_{\mathrm{PS},j}{}^2 \tag{5}$$

As the scattering length density of the solvent does not appear in eq 5, the intensity should be identical for a pair of solutions which differ only in the labeling of the solvent. For a perfectly symmetric copolymer, $f = 0.5$, and in the presence of a perfectly neutral solvent

$$\varphi_{\mathrm{PS},j} = -\varphi_{\mathrm{PI},j} \quad j = 1, 3, 5, \ldots$$

$$\varphi_{\mathrm{PS},j} = \varphi_{\mathrm{PI},j} = -\frac{1}{2}\varphi_{\mathrm{SOL},j} \quad j = 2, 4, 6, \ldots \tag{6}$$

and the peak intensities scale as

$$I(jq^*) \sim (a_{\mathrm{PS}} - a_{\mathrm{PI}})^2 \varphi_{\mathrm{PS},j}{}^2 \quad j = 1, 3, 5, \ldots$$

$$\sim (2(a_{\mathrm{PS}} - a_{\mathrm{SOL}})^2 + 2(a_{\mathrm{PI}} - a_{\mathrm{SOL}})^2 - (a_{\mathrm{PS}} - a_{\mathrm{PI}})^2)\varphi_{\mathrm{SOL},j}{}^2 \quad j = 2, 4, 6, \ldots \tag{7}$$

The calculated contrast factors referenced to the styrene monomer volume, $(a_\alpha - a_\beta)^2$, are listed in Table 2.

The scattered intensity for a $\phi = 0.50$ solution of SI(16-19) in *d*-toluene is shown in Figure 1, for selected temperatures from 10 to 75 °C. The scattering is dominated by the copolymer structure factor peak, centered near $q^* \approx 0.025$ Å^{-1}. The intensity increases, and the peak narrows, as T decreases, as expected. In fact, the ODT is located between 37 and 45 °C, as evident in this figure from the sharp increase in peak width, and confirmed by a plot of $I(q^*)^{-1}$ vs T^{-1} (not shown). This result is also anticipated quantitatively by the expression for ϕ_{ODT} reported previously.[13] In Figure 2 we compare the scattering for this solution and one with the protonated solvent, at 20 °C. (The T dependence of the scattering for the *h*-toluene solution indicates the identical T_{ODT}.) The scattering profiles are apparently very similar, and, in particular, the primary peaks overlap quantitatively; this confirms that this peak arises essentially completely from styrene−isoprene correlations. However, there is a distinct second order reflection for *h*-toluene that is virtually absent in the deuterated case, as can be seen in the inset to the figure where the data near $2q^* \approx 0.05$ Å^{-1} are magnified. (The statistical error bars for these data are comparable to the size of the points.) This result is a direct indication of the segregation of the solvent to the styrene−isoprene interface. A similar comparison is shown in Figure 3 for the $\phi = 0.70$ solution at 30 °C. This sample is deeper into the ordered state, and peaks at $2q^*$ and $3q^*$ are clearly evident (see the inset). However, whereas the first-order and third-order peaks have very similar intensities between the two solvents, the second-order peak is markedly stronger for *h*-toluene. This result is also consistent with the segregation of the solvent to the interface. The small difference in the heights of the primary peaks is attributable to a slight partitioning of the solvent into the isoprene-rich microdomains, as will be demonstrated subsequently.

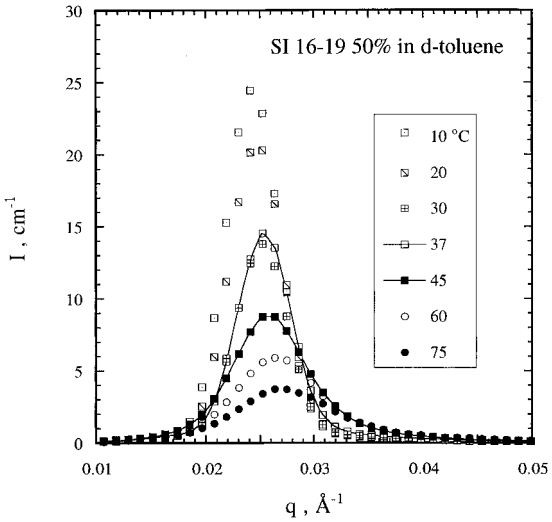

Figure 1. Scattered intensity for SI(16-19) in *d*-toluene, $\phi = 0.50$, at the indicated temperatures. Smooth curves emphasize the data at 37 and 45 °C, which bracket the ODT.

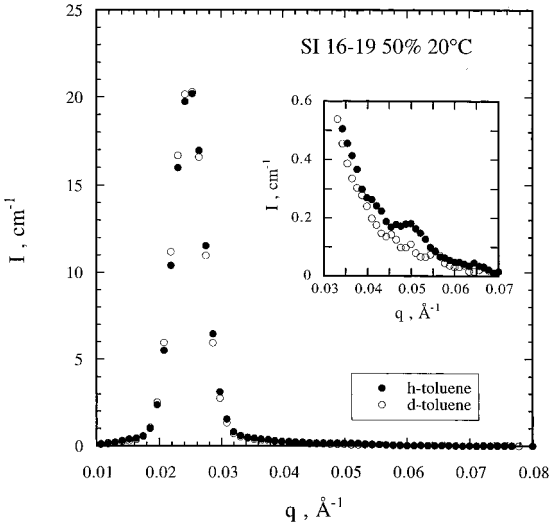

Figure 2. Scattered intensity for SI(16-19) in *d*- and *h*-toluene, $\phi = 0.50$, at 20 °C.

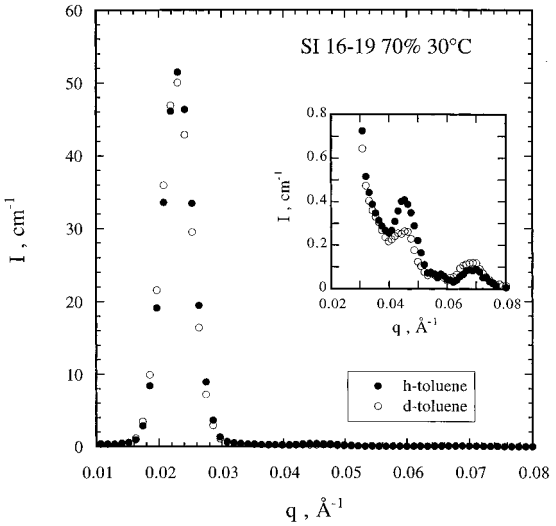

Figure 3. Scattered intensity for SI(16-19) in *d*- and *h*-toluene, $\phi = 0.70$, at 30 °C.

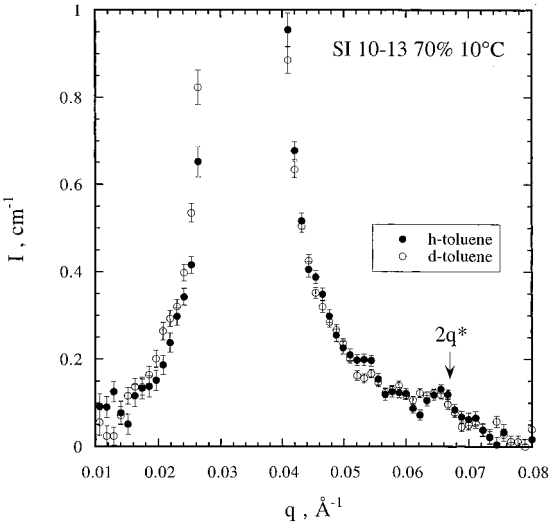

Figure 4. Scattered intensity for SI(10-13) in *d*- and *h*-toluene, $\phi = 0.70$, at 10 °C.

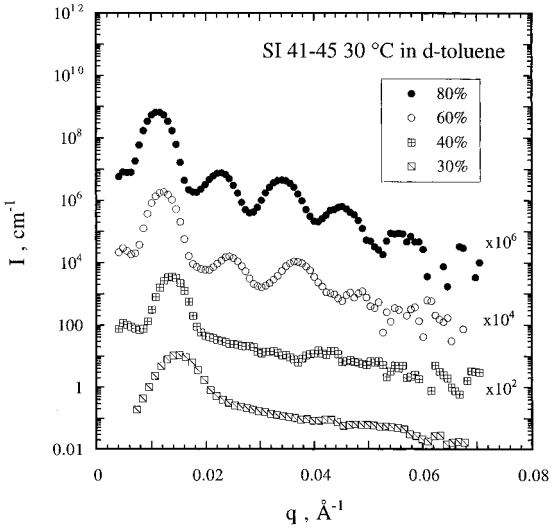

Figure 5. Scattered intensity for SI(41-45) in *d*-toluene at 30 °C, for the indicated concentrations.

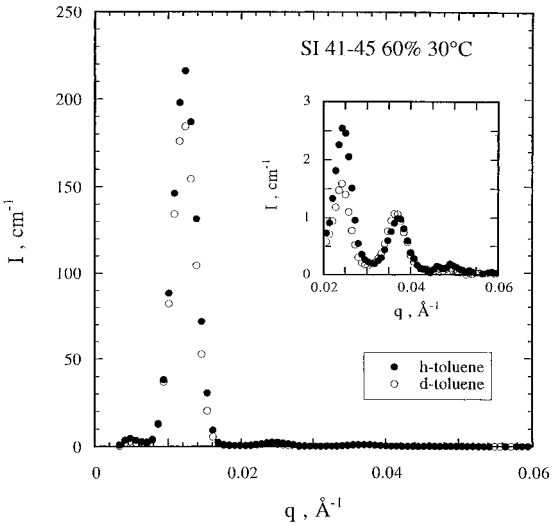

Figure 6. Scattered intensity for SI(41-45) in *d*- and *h*-toluene, $\phi = 0.60$, at 30 °C.

It is interesting to note that it is the *protonated* solvent that gives the larger peak at $2q^*$. For a perfectly symmetric copolymer, eq 7 and the contrast factors in Table 2 indicate that this peak should be about 2000 times larger in the *deuterated* solvent. The copolymer is not exactly symmetric, of course, but the scattering length density of *d*-toluene is so much larger than all of the other components that one might have expected it would dominate the scattering at $2q^*$. This intuition turns out to be quite incorrect, as will be demonstrated subsequently. In fact, the ratio of heights of the second-order peaks in *h*- and *d*-toluene is predicted to be a very strong function of *f*.

The results for solutions of SI(10-13) with $\phi = 0.70$ are shown in Figure 4. The scale is selected to emphasize the data in the vicinity of $2q^*$; the intensities of the primary peak agree very well between the two solutions. In this instance the ODT is located near 40 °C, and thus the data correspond to a degree of segregation that is very similar to that of the SI(16-19) solution in Figure 2. However, there is no difference in the scattering near $2q^*$ between the two solvents, within the uncertainty; in fact, a second order peak is not even obviously resolved. The reason for the difference between Figure 2 and Figure 4 is not apparent, but one factor is the absolute solvent concentration. The lower molecular weight polymer requires a smaller solvent concentration to reach the same thermodynamic state, and thus the intensity of solvent scattering is diminished; this hypothesis will also be supported by the calculations presented subsequently.

The data for four concentrations of SI(41-45) in *d*-toluene at 30 °C are shown in Figure 5, with the intensity now on a logarithmic scale. The ODT for this sample occurs at $\phi = 0.31$, and consequently the three higher concentration solutions are ordered. For the highest concentration shown, $\phi = 0.80$, at least five orders of reflections are resolved. These data demonstrate both the increasing degree of segregation with increasing concentration, and the increase in lamellar spacing, L ($=2\pi/q^*$); L, in fact, increases roughly as $\phi^{0.3}$, in agreement with both earlier experiments of Hashimoto and co-workers[11,12] and SCMF theory.[7] Figure 6 shows a direct comparison of the $\phi = 0.60$ solutions in the two solvents. As with the SI(16-19) solution in Figure 3, the odd reflections have intensities that are almost independent of solvent contrast, whereas the even reflections show stronger scattering for the protonated solvent. Again, the slightly higher intensity for the primary peak in the protonated solvent is due to solvent partitioning.

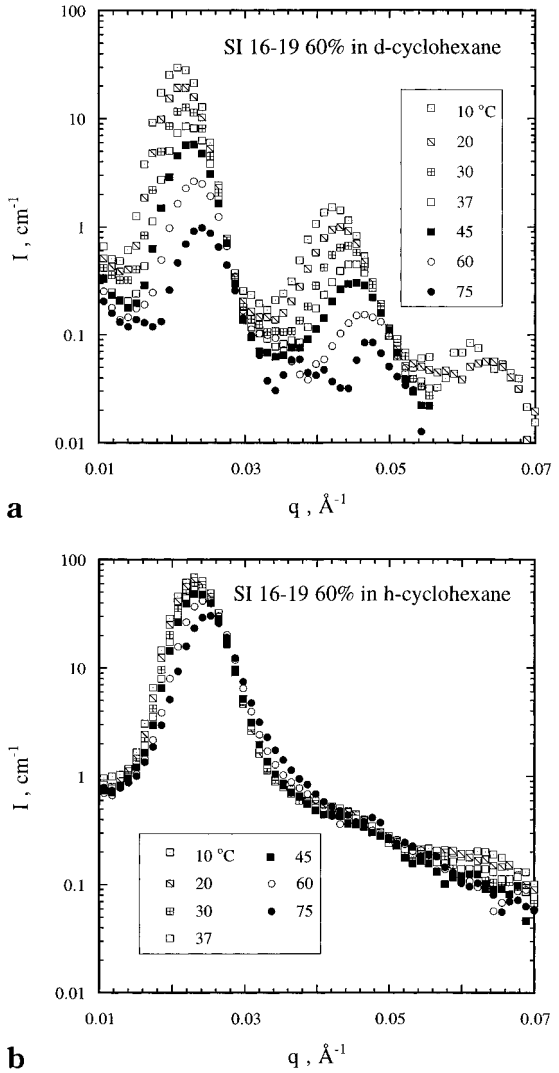

Figure 7. Scattered intensity for SI(16-19), $\phi = 0.60$, at the indicated temperatures in (a) *d*-cyclohexane and (b) *h*-cyclohexane.

Solutions of SI(16-19) in cyclohexane with $\phi = 0.60$ are considered in parts a and b of Figure 7. The polymer concentration is such that these samples are all in the ordered state. The temperature ranges from 10 to 75 °C; it is helpful to recall that *h*-cyclohexane is a Θ solvent for polystyrene at 34.5 °C (39 ± 1 °C for *d*-cyclohexane[18]). Thus one may anticipate increasing preferential solvation of the isoprene-rich domains with decreasing *T*. The scattering profiles are, indeed, markedly different between the two solvents. The deuterated solvent gives a very strong second-order reflection that grows with decreasing *T*. The protonated analog, however, shows no second-order peak at all, except possibly at the lowest *T*. (Note that the intensity axes are logarithmic.) In toluene, it was the protonated solvent that gave a stronger second-order reflection. At the same time, the primary peak intensities are also quite different between the two solutions, whereas they were very similar in toluene. For *h*-cyclohexane, the peak intensity increases from about 30 to 70 cm^{-1} with decreasing *T*, whereas the same quantity varies from 1 to 30 cm^{-1} for *d*-cyclohexane over the same *T* range. This is direct evidence of preferential solvation of one of the domains and of a preferential solvation that varies with temperature.

Theory

In order to gain more quantitative insight into the solvent distribution, we use self-consistent mean-field (SCMF) theory[7,8,19] to calculate equilibrium concentration profiles, and examine the effect of solvent distribution on the peak scattered intensities. This is a mean-field approach, and ignores the effects of, inter alia, chain swelling and fluctuations. Nevertheless, it should provide a reasonable estimate of the solvent distribution in weakly-ordered solutions. We extend the SCMF scheme of Matsen, which was developed to study phase behavior in melts,[20,21] although our approach is very similar to that previously described by Whitmore and Noolandi.[7] The method introduces a series of orthonormal basis functions, $f_j(r)$, which allow us to express any given function, $g(r)$, in terms of the corresponding amplitudes, g_j; i.e., $g(r) = \sum_j g_j f_j(r)$. They reflect the symmetry of the ordered phase being considered and are chosen to be eigenfunctions of the Laplacian operator

$$\nabla^2 f_j(r) = -\lambda_j L^{-2} f_j(r) \tag{8}$$

where L is the length scale for the ordered phase. For lamellae, we use $f_0(r) = 1$ and $f_j(r) = \sqrt{2}\cos(2\pi jx/L)$, $j \geq 1$, as in eq 1, where x is the coordinate orthogonal to the lamellae.

We consider a solution of AB diblock copolymer and solvent, present at average volume fractions ϕ and $1 - \phi$, respectively, and assume the system is incompressible, both locally and globally. Each polymer chain has degree of polymerization N, and A-monomer fraction f. It is assumed that each monomer type has the same statistical segment length b. The local interaction between each pair of units α and β is quantified by the Flory interaction parameter $\chi_{\alpha\beta}$. Each polymer is parametrized with a variable s that increases from 0 to 1 along its length. We assume that the A block starts from $s = 0$ and terminates at $s = f$, which is the A−B junction point. Using this parametrization, it is convenient to define two end-segment copolymer distribution functions, $q_C(r,s)$ and $q_C^+(r,s)$, which are found by integrating all possible configurations subject to the fields, $\omega_A(r)$ and $\omega_B(r)$, for chain segments starting from $s = 0$ to f and from $s = f$ to 1, respectively. The distribution function $q_C(r,s)$ satisfies the modified diffusion equation

$$\frac{\partial q_C}{\partial s} = \begin{cases} \frac{1}{6}Nb^2\nabla^2 q_C - \omega_A q_C & \text{if } s < f \\ \frac{1}{6}Nb^2\nabla^2 q_C - \omega_B q_C & \text{if } s > f \end{cases} \tag{9}$$

and the initial condition, $q_C(r,0) = 1$. The equation for $q_C^+(r,s)$ is similar except that the right-hand side of eq 9 is multiplied by −1, and the initial condition is $q_C^+(r,1) = 1$. Since there is no chain connectivity in the solvent case, the equation governing the solvent distribution function $q_S(r,s)$ becomes

$$\frac{\partial q_S}{\partial s} = -\omega_S(r) q_S \tag{10}$$

In the SCMF theory, the concentrations of the components, $\varphi_\alpha(r)$, as calculated in an ensemble of noninteracting polymers subject to the fields $\omega_\alpha(r)$, α = A, B,

S, are functions for which the total free energy attains a minimum.[19] The minimization of free energy yields the self-consistent equations for the fields and the equilibrium concentrations. The expressions for the fields and the calculation scheme are given in the Appendix.

Once the above amplitudes are determined and the self-consistent equations for the fields are satisfied, the free energy per molecule F is given by

$$\frac{F}{k_B T} = -\phi \ln\left[\frac{q_{C,1}(1)}{\phi}\right] - (1-\phi)N \ln\left[\frac{q_{S,1}(1/N)}{1-\phi}\right] - \sum_i(\omega_{A,i}\varphi_{A,i} + \omega_{B,i}\varphi_{B,i} + \omega_{S,i}\varphi_{S,i}) + \sum_i(\chi_{AB}N\varphi_{A,i}\varphi_{B,i} + \chi_{AS}N\varphi_{A,i}\varphi_{S,i} + \chi_{BS}N\varphi_{B,i}\varphi_{S,i}) \quad (11)$$

which reduces to the Flory−Huggins mean-field free energy functional in the disordered state. For a periodic ordered phase, we minimize the free energy with respect to the lattice spacing L. In general, to determine the most stable phase one compares free energies of different possible phases. However, we neglect the latter step here, since the stable phase is known to be lamellar for the systems studied in this paper. The peak scattered intensities $I(jq^*)$, $j = 1, 2, 3, ...$, are calculated in terms of the mean-field concentration amplitudes and the contrast factors, as in eq 4.

Equation 7 underscored the fact that the distribution of solvent can be understood from the intensities of the even-order peaks. If the solvent concentration profile were uniform and $f = 0.500$, i.e., the amplitudes of all even harmonics vanish, we would expect peak scattered intensities only at odd harmonics. However, no matter how close to the ODT the system is, the calculations indicate that solvent always accumulates at the interface between the A-rich and the B-rich microdomains, and thus at least one even solvent harmonic has a nonzero amplitude. Therefore, finite peak intensities at $2q^*$, $4q^*$, etc., are possible. The more solvent that adsorbs at the interface, the larger the scattered intensities will be. As ϕ decreases from 1 (no solvent), the solvent amplitude, $|\varphi_{S,j}|$, $j = 2, 4, 6, ...$, increases from 0, reaches a maximum, and then decreases to 0 when the system is close to the ODT. Due to this solvent adsorption behavior, we expect a maximum of $I(2jq^*)$ for some $\phi_{ODT} < \phi < 1$, as observed previously by Whitmore and Noolandi.[7] This is illustrated in Figure 8, where $I(2q^*)$ and $\varphi_{s,2}^2$ are plotted as a function of ϕ. These data correspond to a symmetric PS−PI diblock in toluene at 30 °C, with N equal to that for SI(16-19), and $\chi_{PS} = 0.44$, $\chi_{PI} = 0.40$, and $\chi_{PS-PI} = 0.086$. The polymer−solvent interaction parameter values are taken from the literature,[22] and the polymer−polymer value was taken from our previous work.[13] There is indeed a maximum in both the peak intensity and the squared amplitude of the solvent second harmonic, $\varphi_{s,2}^2$, near $\phi \approx 0.5$.

In reality, exactly symmetric block copolymers are elusive, and a perfectly neutral solvent is difficult to find. We therefore examine how the scaling behavior between the scattered intensity and the adsorption amplitude in eq 7 is affected when the solvent is not perfectly neutral or when the copolymer is slightly asymmetric. From Figure 8 we observe that even though the solvent is not perfectly neutral, the scaling of $I(2q^*) \propto \varphi_{s,2}^2$ is still appropriate. However, when the copolymer is slightly asymmetric, this scaling result is

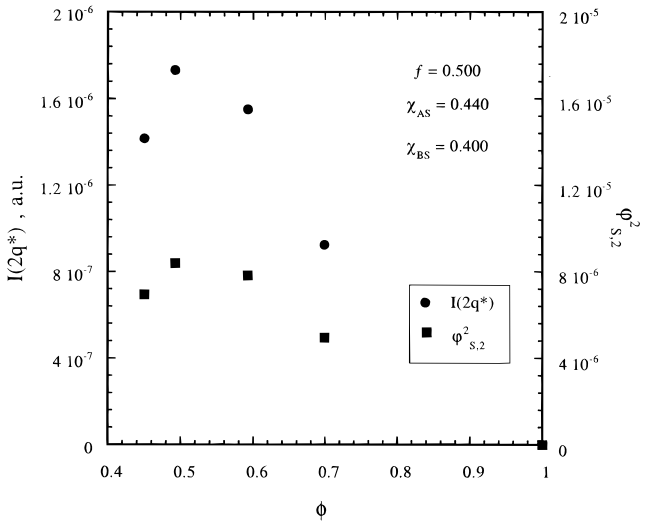

Figure 8. Predicted intensity of the second harmonic peak and the squared solvent second harmonic amplitude as a function of polymer volume fraction, with the indicated parameters.

completely lost, as illustrated in Figure 9. Here we plot the same quantities as in Figure 8, using the same parameters except $f = 0.425$, which corresponds to SI-(16-19). Although there is still a maximum in the solvent amplitude, the peak intensity is monotonic over the same concentration range, as ϕ decreases toward the ODT. Note also that this small change in copolymer composition results in an increase in the scattered intensity by an order of magnitude or more.

The effect of block symmetry on the experimental scattered intensity may be conveniently examined by forming the ratio of peak intensities for protonated and deuterated solvent. For symmetric blocks in a neutral solvent, the ratio of peak intensity

$$\frac{I_h(jq^*)}{I_d(jq^*)} = 1 \quad j = 1, 3, 5, ...$$

$$= \frac{2(a_{PS} - a_{SOL,h})^2 + 2(a_{PI} - a_{SOL,h})^2 - (a_{PS} - a_{PI})^2}{2(a_{PS} - a_{SOL,d})^2 + 2(a_{PI} - a_{SOL,d})^2 - (a_{PS} - a_{PI})^2} \quad (12)$$

$$= \text{constant}, j = 2, 4, 6, ...$$

which shows that although the adsorption of solvent affects the intensity *values* at even-order peaks, the *ratio* of peak intensities remains a constant independent of peak order and concentration. When the copolymer symmetry is broken, this simple result no longer holds. In parts a and b of Figure 10, we plot the first four peak ratios as a function of concentration for $f = 0.425$ and $f = 0.575$, respectively; all other parameters correspond to SI(16-19), as in Figures 8 and 9. In both cases, when there is no solvent ($\phi = 1$), the ratio is always equal to 1. As more solvent is added to the system, the difference between the peak values in *h*- and *d*-toluene becomes more significant. For the isoprene-rich copolymer, the protonated solvent has the larger peaks at $2q^*$ and $4q^*$, as seen experimentally, whereas for the styrene-rich case, the opposite is predicted to hold. Of course, these figures concern ratios of peak intensities; the individual higher order peaks may be too small to observe, for example, near the ODT. Note also the interesting prediction that the primary peak intensity should be

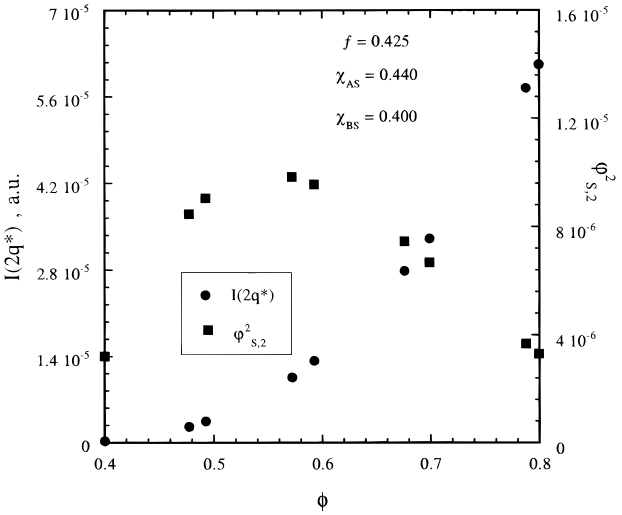

Figure 9. Predicted intensity of the second harmonic peak and the squared solvent second harmonic amplitude as a function of polymer volume fraction, as in Figure 8, but with the copolymer composition $f = 0.425$.

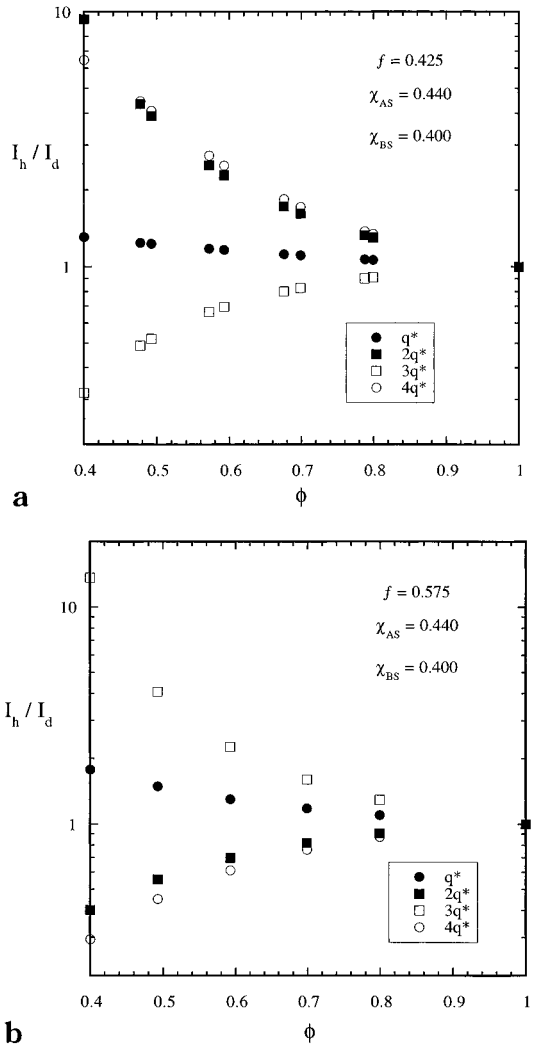

Figure 10. Ratio of predicted peak intensities in *h*-toluene to *d*-toluene, as a function of polymer volume fraction. Parameter values are as in Figures 8 and 9, with (a) $f = 0.425$, and (b) $f = 0.575$.

slightly larger in the protonated solvent, in either case, as the amount of solvent is increased; this is a consequence of the slight solvent selectivity and is observed experimentally (e.g., Figures 3 and 6).

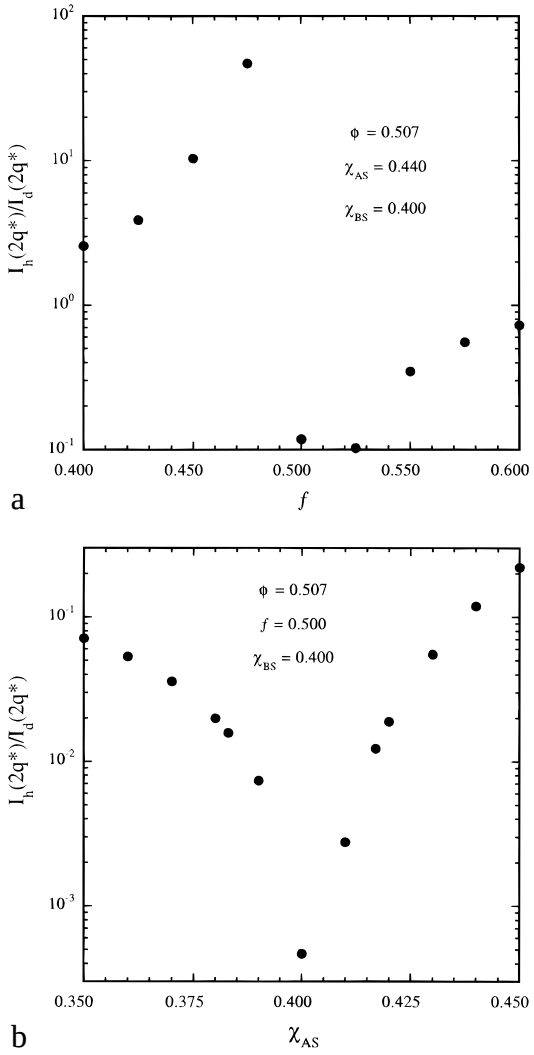

Figure 11. Ratio of predicted second harmonic intensities in *h*-toluene to *d*-toluene (a) as a function of copolymer composition and (b) as a function of the polystyrene−toluene interaction parameter.

The results in Figure 10 indicate a remarkable sensitivity in the intensity ratios for the second harmonic peak, as a function of copolymer composition. For example, consider solutions with $\phi \approx 0.5$. When $f = 0.425$ (Figure 10a), the *h*-toluene peak is a factor of four larger, whereas for $f = 0.575$ (Figure 10b) it is *d*-toluene that gives the larger intensity. Previously, it was noted in the context of eq 7 that for a perfectly neutral solvent and $f = 0.500$, *d*-toluene should give an intensity 3 orders of magnitude larger than *h*-toluene. Accordingly, in Figure 11a we show $I_h(2q^*)/I_d(2q^*)$ as a function of f, for a solution with $\phi \approx 0.5$ and the parameters appropriate to SI(16-19) in toluene. Over the range from $f = 0.4$ to 0.6, for which the samples may be assumed to be lamellar, the intensity ratio varies by 3 orders of magnitude, and in a decidedly nonmonotonic fashion. This remarkable result is a consequence of the location of the solvent concentration maximum near the interface between the PS-rich and PI-rich domains, i.e., in the region where the scattering length density varies most strongly with position. Accordingly, small changes in solvent distribution lead to large changes in relative scattering power. This result even suggests that one could employ SANS with differential solvent contrast as a means of measuring copolymer composition with greater precision than typically obtained by spectroscopic means! However, it is important to emphasize

Table 3. Comparison of Experimental and Calculated Peak Intensities for SI(16-19) in Toluene at 30 °C[a]

ϕ_h, ϕ_d	peak	I_h (theory)	I_d (theory)	I_h (exptl)	I_d (exptl)	I_h/I_d (theory)	I_h/I_d (exptl)
0.477, 0.493	q^*	5.15×10^{-5}	4.7×10^{-5}	14.4	13.7	1.10	1.05
0.572, 0.592	q^*	9.30×10^{-4}	8.82×10^{-4}	31.7	34.1	1.05	0.93
	$2q^*$	2.67×10^{-5}	1.34×10^{-5}	0.24	0.17	1.99	1.41
0.676, 0.699	q^*	1.46×10^{-3}	1.43×10^{-3}	51.6	50.4	1.02	1.02
	$2q^*$	4.81×10^{-5}	3.31×10^{-5}	0.41	0.26	1.45	1.58
	$3q^*$	2.14×10^{-5}	3.07×10^{-5}	0.09	0.12	0.70	0.75
0.788, 0.799	q^*	2.12×10^{-3}	2.06×10^{-3}	52.6	66.0	1.03	0.80
	$2q^*$	7.64×10^{-5}	6.13×10^{-5}	0.49	0.49	1.25	1.00
	$3q^*$	4.41×10^{-5}	5.16×10^{-5}	0.17	0.20	0.85	0.85

[a] Experimental intensities in units of cm^{-1}; theoretical intensities in arbitrary units.

that although the relative peak intensities vary strongly, it is not guaranteed that both peaks will have sufficient scattering power to be accurately characterized.

The sensitivity of the relative peak intensities also applies when varying the degree of solvent selectivity, as indicated in Figure 11b. Here the interaction parameter for the "styrene" component (nominally 0.44) is varied from 0.35 to 0.45, holding the "isoprene" component value at 0.40. There is a very sharp minimum in the relative intensity at the point of exact solvent neutrality. Consequently, this suggests a possible method to quantify small degrees of selectivity of common good solvents for block copolymers.

In Table 3, we compare the scattered intensities from the SANS experiments with the calculated results for SI(16-19) in toluene at 30 °C. The calculated intensity ratios, $I_h(jq^*)/I_d(jq^*)$, are in good agreement with the experimental results at any peak and any concentration studied here, especially with regard to trends. Although the solutions made as hydrogenous and deuterous pairs are not at precisely the same volume fractions, this has a negligible effect on the calculations. Especially when the sensitivity of the intensity ratios to composition and selectivity is considered, the agreement is remarkable; no attempt has been made to adjust the values of f or χ to optimize the fit (however, the exact values of the interaction parameters are much less important than the difference between them). From this success of the SCMF approach, therefore, we may conclude that the failure of the dilution approximation in concentrated symmetric block copolymer solutions is not directly related to the distribution of solvent.

In Figure 12a we show the calculated composition profiles (using the first 20 harmonics) for the three components, when $\phi = 0.477$ and $T = 30$ °C; this corresponds to the solutions for which the scattering curves are given in Figures 1 and 2. Even on this scale, the inhomogeneity of the solvent distribution is clear; toluene collects at the styrene−isoprene interface and is very slightly preferentially absorbed into the isoprene-rich domains. The solvent profiles as a function of ϕ are shown in Figure 12b, corresponding to the four concentrations of SI(16-19) examined. With increasing polymer concentration, the solvent peak at the interface sharpens, as expected based on the increasing degree of segregation, and the effect of solvent selectivity decreases slightly.

We now consider SI(16-19) in the selective solvent cyclohexane, and initially employ the following interaction parameters: $\chi_{PI-CYC} = 0.394$,[23] and $\chi_{PS-CYC} = -0.556 + 324.3/T$.[24] For simplicity, the interaction parameters are taken to be independent of solvent labeling, and independent of T for PI; of course, including a T dependence of χ for PS is essential. The T dependence for a given solvent may be considered by forming the ratio $I(T)/I(10$ °C), as illustrated in Table 4

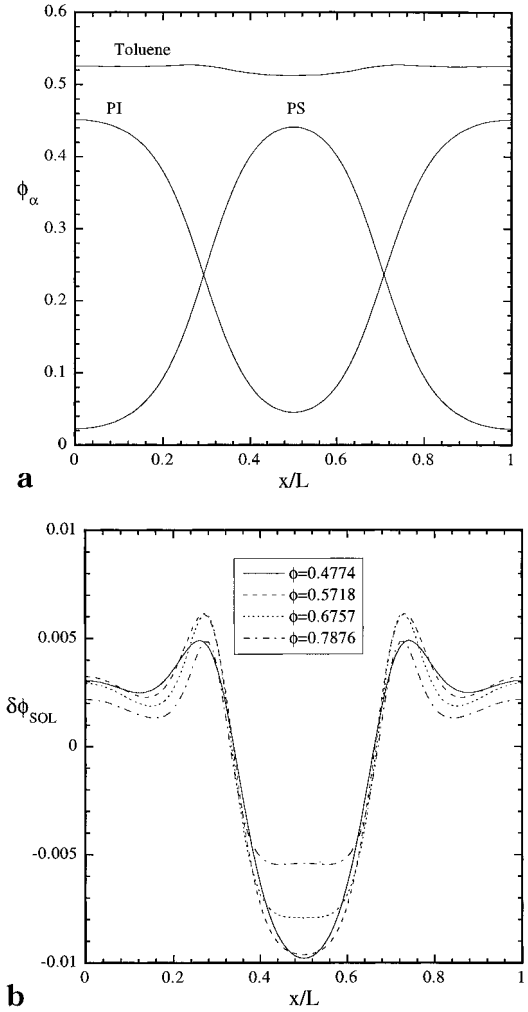

Figure 12. (a) Predicted composition profiles corresponding to solutions of SI(16-19) in toluene at 30 °C, $\phi = 0.48$, as shown in Figures 1 and 2, and (b) the solvent profiles as a function of ϕ.

for the primary peak. For the protonated solvent, the agreement is excellent; however, for the deuterated solvent, the theory and experiment disagree dramatically, with the two ratios having opposite dependences on T. This result is perhaps not too surprising, given the remarkable parametric sensitivity of the SCMF calculations when the contrast factors are included. However, it is not possible to capture the experimental I_h/I_d ratios or the T dependences of I for both solvents concurrently by minor variations in f or χ. Rather, what seems to be required is introduction of a surprisingly large difference between the interaction parameters for the two solvents. For example, if the χ_{PS-CYC} expression above is retained, then χ_{PI-CYC} must be decreased to *ca.* 0.07; although this is not physically unreasonable, it is rather unsettling, as empirically most polymer/good

Table 4. Comparison of Experimental and Calculated Primary Peak Intensities for SI(16-19) in Cyclohexane[a]

			$I/I(10)_h$			$I/I(10)_d$			I_h/I_d	
T, °C	I_h (exptl)	I_d (exptl)	(theory)[b]	(theory)[c]	exptl	(theory)[b]	(theory)[c]	exptl	(theory)[c]	exptl
10	67.6	30.2	1.00	1.00	1.00	1.00	1.00	1.00	2.23	2.24
20	62.2		0.91		0.92					
30	56.7	12.8	0.81	0.90	0.84	2.84	0.46	0.43	4.43	4.43
37	52.1		0.75		0.77					
45	48.7		0.69		0.72					
60	41.2	2.7	0.58	0.56	0.61	5.53	0.08	0.09	15.39	15.26

[a] Experimental intensities in units of cm^{-1}; theoretical intensities in arbitrary units. [b] Using literature values for the polymer−solvent interaction parameters. [c] Using 0.906, 0.832, and 0.616 for χ_{PS-CYC} at 10, 30, and 60 °C, respectively.

solvent χ values tend to be greater than 0.3.[25] The same success can be achieved by maintaining χ_{PI-CYC} at 0.394 and increasing χ_{PS-CYC} up to 0.6 to 1; the resulting comparisons of the primary peak intensites are also shown in Table 4. Such magnitudes for χ_{PS-CYC} might appear to violate the definition of the Θ point, but in fact, this is not so. As pointed out by Sanchez, when χ depends on concentration, the values determined by different experiments will not be the same. Furthermore, the χ_{PS-CYC} appropriate for use in the free energy expression and for the concentrations considered here is in the vicinity of 1.[26] As can be seen from Table 4, excellent agreement is found for the temperature dependence of the primary peak intensity in both *h*- and *d*-cyclohexane, and for the ratio of the intensities between the two solvents. The resulting composition profiles for 10 and 60 °C (using 18 harmonics) are shown in parts a and b of Figure 13, respectively. The strong partitioning of the solvent is evident, as is the substantial temperature dependence of the effect. However, it turns out that these profiles do not capture the behavior of the second-order peaks accurately, and thus the applicability of the SCMF approach is not firmly established in this instance.

The strong dependence of $I(q^*)$ on both solvent labeling and T suggests a more direct approach to estimating the preferential solvation of the PI domains. We can assume that the first harmonic of the solvent profile is simply proportional to that of the PI component

$$\varphi_{CYC,1} = \alpha\varphi_{PI,1} \tag{13}$$

which permits the ratio $I_h(q^*)/I_d(q^*)$ to be written as a function of α and the contrast factors alone. The result is shown in Figure 14; the ratio is very sensitive to α, particularly over the range from 0.1 to 0.4 (see inset). As increasing T should correspond to decreasing α, i.e. the solvent becomes less selective, the experimental results correspond to the right side of the peak in Figure 14. Thus, the intensity ratio is 18.3 at 60 °C, giving $\alpha \approx 0.28$, and at 10 °C the ratio of 2.2 implies that $\alpha \approx 0.45$. These values are consistent with the results in Figure 13.

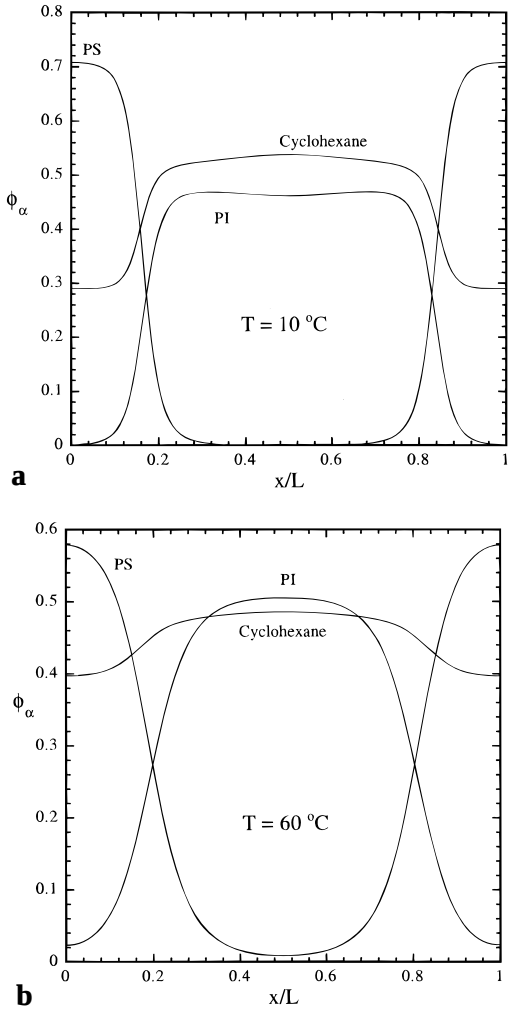

Figure 13. Predicted composition profiles corresponding to solutions of SI(16-19) in cyclohexane at (a) 10 °C and (b) 60 °C.

Summary

We have employed SANS on solutions of lamellar-forming styrene−isoprene diblock copolymers to examine the distribution of solvent. By comparison of the scattering profiles for two solutions of equal polymer concentration, one with protonated and the other with deuterated solvent, it is possible to assess both the selectivity of the solvent and its tendency to collect at the interface between microdomains. To a first approximation, differences in the scattered intensity of the main structure factor peak (and higher order, odd-numbered reflections) between the two solvents reflect preferential partitioning of the solvent into one domain, whereas differences in the even-numbered peaks indicate solvent segregation to the interface. For a perfectly symmetric diblock in a perfectly neutral solvent, these statements would be exact. However, the quantitative effects are rather sensitive to small variations in both copolymer composition and solvent selectivity. A self-consistent mean-field calculation scheme has been employed to estimate the composition profiles and to explore the dependence of the scattered intensity on the relevant solution variables.

For toluene, which is a nearly neutral good solvent, the calculated ratios of peak intensities between the two solvents (h and d) are in very good agreement with the

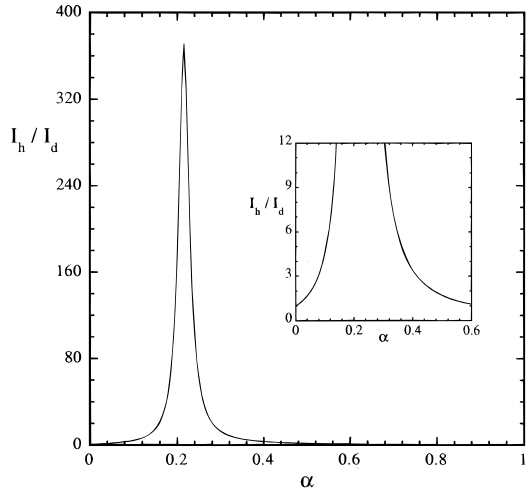

Figure 14. Ratio of predicted primary peak intensities for SI(16-19) in *h*-cyclohexane to *d*-cyclohexane, as a function of the ratio of the amplitude of the solvent first harmonic to that of polyisoprene.

data, suggesting that for polymer concentrations above about 50%, effects of chain swelling (ignored in the calculations) are modest. The experiments show that toluene does collect at the interface between styrene- and isoprene-rich domains, to an extent anticipated quantitatively by the theory. Thus, we may discard solvent distribution as a contribution to the failure of the dilution approximation to predict the N dependence of ϕ_{ODT} for lamellar copolymer solutions. In the selective solvent cyclohexane, the data indicate a strong and highly temperature-dependent preferential swelling of the isoprene-rich microdomains. The detailed calculations can only describe these data by incorporating unexpectedly large differences in the interaction parameters for the two polymers in cyclohexane, and even then, they cannot simultaneously capture the behavior of the second-order peaks; the underlying significance of this observation remains to be established. However, a more direct estimation confirms that cyclohexane partitions substantially into the PI-rich microdomains. Taken as a whole, the calculations indicate that the general approach of SANS from copolymer solutions with differential solvent contrast is very promising. Under appropriate circumstances, the ratio of peak intensities between labeled and unlabeled solvents can change by an order of magnitude or more, upon very minor changes in copolymer composition and/or solvent selectivity.

Acknowledgment. This work was supported by the National Science Foundation, through Grant DMR-9528481, and by the Center for Interfacial Engineering, an NSF-supported Engineering Research Center at the University of Minnesota. We appreciate helpful discussions with M. Matsen about the calculations and the assistance of C. Glinka and S. Kline with the SANS measurements.

Appendix

Utilizing the amplitudes corresponding to the basis functions as in eq 1, the amplitudes of the fields have to satisfy

$$\omega_{A,i} - \omega_{S,i} = \chi_{AB}N\varphi_{B,i} + \chi_{AS}N\varphi_{S,i} - \chi_{AS}N\varphi_{A,i} - \chi_{BS}N\varphi_{B,i} \quad i = 0, 1, 2, \ldots$$

$$\omega_{B,i} - \omega_{S,i} = \chi_{AB}N\varphi_{A,i} + \chi_{BS}N\varphi_{S,i} - \chi_{AS}N\varphi_{A,i} - \chi_{BS}N\varphi_{B,i} \quad i = 0, 1, 2, \ldots$$

$$\varphi_{A,i} + \varphi_{B,i} + \varphi_{S,i} = \delta_{i0} \quad i = 0, 1, 2, \ldots \qquad \text{(A-1)}$$

In turn, the amplitudes of the concentrations of A, B, and S are expressed in terms of the distribution functions

$$\varphi_{A,i} = \frac{\phi}{q_{C,1}(1)}\sum_{j,k}\Gamma_{ijk}\int_0^f q_{C,j}(s)q^+_{C,k}(s)\,ds$$

$$\varphi_{B,i} = \frac{\phi}{q_{C,1}(1)}\sum_{j,k}\Gamma_{ijk}\int_f^1 q_{C,j}(s)q^+_{C,k}(s)\,ds$$

$$\varphi_{S,i} = q_{S,i}\left(\frac{1}{N}\right) \qquad \text{(A-2)}$$

where

$$\Gamma_{ijk} = \frac{1}{V}\int f_i(r)f_j(r)f_k(r)\,dr \qquad \text{(A-3)}$$

and the modified diffusion eqs 9 and 10 in terms of $q_{C,i}(s)$, $q^+_{C,i}(s)$, and $q_{S,i}(s)$ become

$$\frac{\partial q_{C,i}}{\partial s} = \begin{cases} \sum_j A_{ij}\, q_{C,j} & \text{if } s < f \\ \sum_j B_{ij}\, q_{C,j} & \text{if } s > f \end{cases} \qquad \text{(A-4)}$$

(the equation for $q^+_{C,i}(s)$ is similar except that the right-hand side is multiplied by -1) and

$$\frac{\partial q_{S,i}}{\partial s} = \sum_j C_{ij}\, q_{S,j} \qquad \text{(A-5)}$$

with the initial conditions, $q_{C,i}(s = 0) = \delta_{i,0}$, $q^+_{C,i}(s = 1) = \delta_{i0}$ and $q_{S,i}(s = 0) = \delta_{i0}$. The matrices A_{ij}, B_{ij}, and C_{ij} are given by

$$A_{ij} = -\frac{Nb^2}{6L^2}\lambda_i\delta_{ij} - \sum_k \omega_{A,k}\Gamma_{ijk}$$

$$B_{ij} = -\frac{Nb^2}{6L^2}\lambda_i\delta_{ij} - \sum_k \omega_{B,k}\Gamma_{ijk}$$

$$C_{ij} = -\sum_k \omega_{S,k}\Gamma_{ijk} \qquad \text{(A-6)}$$

References and Notes

(1) Lin, H.; Steyerl, A.; Satija, S. K.; Karim, A.; Russell, T. P. *Macromolecules* **1995**, *28*, 1470.
(2) Tirrell, M.; Levicky, R.; Koneripalli, N.; Satija, S. K.; Gallagher, P. D.; Ankner, J. F.; Kulasekere, R.; Kaiser, H. *Macromolecules*.
(3) Noolandi, J.; Hong, K. M. *Ferroelectrics* **1980**, *30*, 117.
(4) Hong, K. M.; Noolandi, J. *Macromolecules* **1983**, *16*, 1083.
(5) Fredrickson, G. H.; Leibler, L. *Macromolecules* **1989**, *22*, 1238.
(6) Olvera de la Cruz, M. *J. Chem. Phys.* **1989**, *90*, 1995.
(7) Whitmore, M. D.; Noolandi, J. *J. Chem. Phys.* **1990**, *93*, 2946.

(8) Helfand, E.; Tagami, Y. *J. Chem. Phys.* **1972**, *56*, 3592.
(9) Joanny, J.-F.; Leibler, L.; Ball, R. *J. Chem. Phys.* **1984**, *81*, 4640.
(10) Broseta, D.; Leibler, L.; Joanny, J.-F. *Macromolecules* **1987**, *20*, 1935.
(11) Shibayama, M.; Hashimoto, T.; Hasegawa, H.; Kawai, H. *Macromolecules* **1983**, *16*, 1427.
(12) Hashimoto, T.; Shibayama, M.; Kawai, H. *Macromolecules* **1983**, *16*, 1093.
(13) Lodge, T. P.; Pan, C.; Jin, X.; Liu, Z.; Zhao, J.; Maurer, W. W.; Bates, F. S. *J. Polym. Sci., Polym. Phys. Ed.* **1995**, *33*, 2289.
(14) Guenza, M.; Schweizer, K. S. *Macromolecules* **1997**, *30*, 4205.
(15) Pan, C.; Maurer, W.; Liu, Z.; Lodge, T. P.; Stepanek, P.; von Meerwall, E. D.; Watanabe, H. *Macromolecules* **1995**, *28*, 1643.
(16) Hamersky, M. W.; Tirrell, M.; Lodge, T. P. *J. Polym. Sci., Polym. Phys. Ed.* **1996**, *34*, 2899.
(17) Higgins, J. S.; Benoit, H. C. *Polymers and Neutron Scattering*; Clarendon Press: Oxford, England, 1994.
(18) Strazielle, C.; Benoit, H. C. *Macromolecules* **1975**, *8*, 203.
(19) Hong, K. M.; Noolandi, J. *Macromolecules* **1981**, *14*, 727.
(20) Matsen, M. W. *Phys. Rev. Lett.* **1995**, *74*, 4225.
(21) Matsen, M. W. *Macromolecules* **1995**, *28*, 5765.
(22) Sheehan, C. J.; Bisio, A. L. *Rubber Chem. Technol.* **1966**, *39*, 149.
(23) Bristow, G. M.; Watson, W. F. *Trans. Faraday Soc.* **1958**, *54*, 1731.
(24) Shultz, A. R.; Flory, P. J. *J. Am. Chem. Soc.* **1952**, *74*, 4760.
(25) *Polymer Handbook*, 3rd ed.; Brandrup, J., Immergut, E. H., Eds.; John Wiley & Sons: New York, 1989.
(26) Sanchez, I. C. *Polymer* **1989**, *30*, 471.

MA970720Z